 Communications in Theoretical Physics

Commun. Theor. Phys. **75** (2023) 085201 (8pp) https://doi.org/10.1088/1572-9494/ace038

Searching for a_0(980)-meson parton distribution function

Zai-Hui Wu, Hai-Bing Fu*, Tao Zhong, Yu Chen and Ya-Hong Dai

Department of Physics, Guizhou Minzu University, Guiyang 550025, China

E-mail: fuhb@cqu.edu.cn and zhongtao1219@sina.com

Received 9 March 2023, revised 21 June 2023
Accepted for publication 21 June 2023
Published 1 August 2023

Abstract

In this paper, we calculate the scalar a_0(980)-meson leading-twist wave function by using the light-cone harmonic oscillator model (LCHO), where the model parameters are determined by fitting the ξ-moments $\langle\xi^n_{a_0}\rangle_\zeta$ of its light-cone distribution amplitudes. Then, the a_0(980)-meson leading-twist light-cone distribution amplitudes with three different scales $\zeta = (1.0, 2.0, 5.2)$ GeV are given. After constructing the relationship between the a_0(980)-meson leading-twist parton distribution functions/valence quark distribution function and its LCHO wave function, we exhibit the $q^{a_0}(x, \zeta)$ and $xq^{a_0}(x, \zeta)$ with different scales. Furthermore, we also calculate the Mellin moments of the a_0(980)-meson's valence quark distribution function $\langle x^n q^{a_0}\rangle_\zeta$ with $n = (1, 2, 3)$, i.e. $\langle xq^{a_0}\rangle_{\zeta_5} = 0.027$, $\langle x^2q^{a_0}\rangle_{\zeta_5} = 0.018$ and $\langle x^3q^{a_0}\rangle_{\zeta_5} = 0.013$. Finally, the scale evolution for the ratio of the Mellin moments $x^n_{a_0}(\zeta, \zeta_k)$ are presented.

Supplementary material for this article is available online

Keywords: parton distribution functions, light-cone distribution amplitudes, light scalar meson, light-cone harmonic oscillator model

(Some figures may appear in colour only in the online journal)

1. Introduction

The exploration of quark-gluon structure hadrons has been a cutting-edge issue across particle physics and medium-high energy nuclear physics in recent years. Among them, quarks and gluons, called partons, are the fundamental degrees of freedom of quantum chromodynamics (QCD). Although the parton can not be directly observed, the QCD factorization theorem allows one to express the information of the parton inside the nucleon in terms of nonperturbative functions [1]. At the same time, the parton distribution function (PDF) is considered to be the most important nonperturbative function, which plays an important role in describing the non-perturbative QCD for the internal structure of hadronic bound states [2]. In addition, it also gives the probability of finding quarks and gluons inside a hadron. In the infinite momentum coordinate system [3–6], PDFs are used to describe the one-dimensional momentum distributions of quarks and gluons. Therefore, the internal structure of hadrons can be studied by calculating the meson's PDF.

The PDF constitutes the basic limit of the Higgs boson characterization in the matter of coupling and is the main system for Standard Model (SM) measurements such as W-boson mass. Also, it is still the largest uncertainty outside the production of SM heavy particles so it has important phenomenological value. The MMHT [7], CT [8], NNPDF [9], HERAPDF [10], and JAM [11] have made substantial efforts to determine PDFs and their uncertainties. The pion deemed to the lightest bound state of QCD and kaon has been predicted by many theoretical calculations, chiral-quark model [12–14], Nambu–Jona–Lasinio model [15], light-front holographic QCD (LHFQCD) [16–19], light front quantization [20–22], maximum entropy method [23, 24], Dyson–Schwinger equations (DSEs) [25–35] and lattice QCD [36–45] for the valence quark PDF. Meanwhile, PDFs can be attained directly from the light-front wave function (LFWF), which has been researched via the Bethe–Salpeter wave functions within covariant DSEs, LHFCD and BLFQ. The scalar mesons below 1 GeV are an interesting field to

* Author to whom any correspondence should be addressed.

researchers, especially for $a_0(980)$ state. Its internal structure has some pictures, such as quark–antiquark states [46–51], tetraquark states [52–57], two-meson molecule-bound states [58–62] and hybrid states [63]. In this paper, we mainly take the $a_0(980)$ state as the quark–antiquark picture. Until now, there is less research about the scalar meson $a_0(980)$ PDFs. Thus, in order to understand the internal structure of the $a_0(980)$-meson, the $a_0(980)$-meson parton distribution function will be studied in this paper.

One of the earliest predictions for the $J = 0$ meson valence–quark distribution function for large-x behaviour within the QCD improved parton model [64–66], has the following expression:

$$q^{\rm M}(x;\zeta) \overset{x\simeq 1}{=} c(\zeta)(1-x)^{\beta_\zeta},\ \ \beta_\zeta = 2, \tag{1}$$

where $c(\zeta)$ is independent of x and the ζ stands for the resolving scale. The symbol 'M' stands for each $J = 0$ meson. Since the meson's PDF can be obtained directly from its wave function (WF), a more accurate $a_0(980)$-meson WF is crucial for us to determine its PDF. The light-cone harmonic oscillator model (LCHO) for the light or heavy meson WF is mainly based on the Brodsky–Huang–Lepage (BHL) prescription [67], which has been used in many cases [68–76]. For this model, the total WF can be separated into spin-space WF $\chi_{\rm M}^{\lambda_1\lambda_2}(x,\boldsymbol{k}_\perp)$ and spatial wave function $\psi_{\rm M}^{\rm R}(x,\boldsymbol{k}_\perp)$. The spatial WF is divided into the x-dependence part and the $\boldsymbol{k}_\perp$-dependence part for calculation. The $\boldsymbol{k}_\perp$-dependence part derives from the approximate bound-state solution and the x-dependence part $\varphi_{\rm M}(x)$ can be expanded in Gegenbauer polynomials.

Furthermore, the meson light-cone distribution amplitudes (LCDAs) can also be related to its WF, which leads to the indirect relationship between meson LCDAs and PDFs. In many applications of LCDAs, one usually takes a truncated form to determine DAs, involving only the first few terms of the Gegenbauer expansion series. With the increase of n, there will exist dimensional anomalies which lead to spurious oscillations. In addition, one of the most important factors is the unreliability of the higher-order Gegenbauer moments. In order to improve this phenomenon, one can adopt the LCHO model to deal with the meson LCDAs. In our previous works [76, 77], meson leading-twist LCDAs are studied by using the LCHO model, and then the model parameters are determined by fitting moments with the least squares method. Therefore, we will study the $a_0(980)$-meson PDFs based on BHL prescription in this paper.

2. Theoretical framework

If one wants to use the typical probability expression of quantum mechanics to describe the measurable properties of a given hadron, the first thing one needs to do is find the WF. Each element of the WF Fock-space decomposition represents the probability amplitude of finding n components in the hadron. However, the PDFs describe the longitudinal momentum distribution parton of the hadron. To derive the $a_0(980)$-meson leading-twist PDF, the following expression can be used [34]

$$q^{a_0}(x,\zeta) = \int_{|\boldsymbol{k}_\perp|^2\leqslant\zeta^2} {\rm d}^2\boldsymbol{k}_\perp |\psi_{a_0}(x,\boldsymbol{k}_\perp)|^2, \tag{2}$$

where $\psi_{a_0}(x,\boldsymbol{k}_\perp)$ is WF and ζ stands for the scale. In order to calculate the PDF, the connection between distribution amplitudes and distribution function can be established to achieve the purpose. Exploiting this relationship, one can predict $a_0(980)$-meson leading-twist PDFs with the LCHO model based on the BHL description [67, 75, 78]. The LCHO model of the $a_0(980)$-meson leading-twist WF is denoted by

$$\psi_{a_0}(x,\boldsymbol{k}_\perp) = \sum_{\lambda_1\lambda_2} \chi_{a_0}^{\lambda_1\lambda_2}(x,\boldsymbol{k}_\perp)\psi_{a_0}^{\rm R}(x,\boldsymbol{k}_\perp), \tag{3}$$

where $\boldsymbol{k}_\perp$ is transverse momentum and the symbol 'R' means that $\psi_{a_0}^{\rm R}(x,\boldsymbol{k}_\perp)$ is the spatial wave function in coordinate form. The LCHO model consists of the spin wave function $\chi_{a_0}^{\lambda_1\lambda_2}(x,\boldsymbol{k}_\perp)$ and $\psi_{a_0}^{\rm R}(x,\boldsymbol{k}_\perp)$ as the space wave function. Furthermore, λ_1 and λ_2 are the helicities of the two constituent quarks. The spin-space WF $\chi_{a_0}^{\lambda_1\lambda_2}(x,\boldsymbol{k}_\perp)$ comes from the Wigner–Melosh rotation. The different forms for $\lambda_1\lambda_2$ can also be found in [75]. Thus the sum of the spin-space WF has the following form

$$\sum_{\lambda_1\lambda_2} \chi_{a_0}^{\lambda_1\lambda_2}(x,\boldsymbol{k}_\perp) = \frac{m_q^2}{\sqrt{\boldsymbol{k}_\perp^2 + m_q^2}}, \tag{4}$$

with $m_q = m_u = m_d$. On the other hand, the BHL description proposed the assumption that the valence Fock WF depends only on the energy variable ϵ outside the shell. At the same time, the connection between the equal-time WF in the rest frame and the light-cone wave function in the infinite frame by equating the energy propagator $\epsilon = M^2 - (\sum_{i=1}^n k_i)^2$ is proposed. The propagators in different frames are as follows

$$\begin{aligned} \epsilon_1 &= M^2 - \left(\sum_{i=1}^n q_i^0\right)^2, \qquad \sum_{i=1}^n \boldsymbol{q}^i = 0\\ \epsilon_2 &= M^2 - \left(\sum_{i=1}^n \frac{\boldsymbol{k}_{\perp i}^2 + m_i^2}{x_i}\right), \sum_{i=1}^n \boldsymbol{k}_{\perp i}^2 = 0,\\ &\qquad\qquad\qquad\qquad\qquad\quad \sum_{i=1}^n x^i = 1, \end{aligned} \tag{5}$$

where the index i is represented as the parton, when $i = 1$, it is represented as the u-quark, and $i = 2$ is represented as the d-quark. For the two-particle system, one can get

$$\boldsymbol{q}^2 \leftrightarrow \frac{\boldsymbol{k}_{\perp i}^2 + m_q^2}{4x(1-x)} - m_q^2, \tag{6}$$

where $q_1^0 = q_2^0$. Besides, the rest frame wave function $\psi_{\rm CM}(\boldsymbol{q})$ and the light-cone wave function $\psi_{\rm LC}(x,\boldsymbol{k})$ might be related in some way [75]

$$\psi_{\rm CM}(\boldsymbol{q}^2) \leftrightarrow \psi_{\rm LC}\left(\frac{\boldsymbol{k}_\perp^2 + m_q^2}{4x(1-x)} - m_q^2\right). \tag{7}$$

In this paper, based on the approximation for the bound state solution of the meson quark model, the WF of the harmonic oscillator model in the rest frame is expressed as

$$\psi_{\rm CM}(\boldsymbol{q}^2) = A\exp\left(-\frac{\boldsymbol{q}^2}{2\beta^2}\right). \quad (8)$$

Combining equations (7) and (8), the spatial WF for $a_0(980)$-meson can be obtained

$$\psi^{\rm R}_{a_0}(x, \boldsymbol{k}_\perp) \propto \exp\left[-\frac{\boldsymbol{k}_\perp^2 + m_q^2}{8\beta_{a_0}^2 x\bar{x}}\right]. \quad (9)$$

With $\bar{x} = 1 - x$ from [76], we can get a $a_0(980)$-meson spatial WF,

$$\psi^{\rm R}_{a_0}(x, \boldsymbol{k}_\perp) = A_{a_0}\varphi_{a_0}(x)\exp\left[-\frac{\boldsymbol{k}_\perp^2 + m_q^2}{8\beta_{a_0}^2 x\bar{x}}\right], \quad (10)$$

where the free parameters A_{a_0} stands for normalization constant, the harmonious parameter β_{a_0} can determine the transverse distribution amplitudes of meson WF and $\varphi_{a_0}(x)$ is crucial for determining the WF longitudinal distribution amplitude. It can be expressed in terms of the first few terms of the Gegenbauer moment polynomials since the $a_0(980)$-meson leading-twist amplitude is antisymmetric under $u \to (1-u)$ transition in the $SU_f(3)$ limit.

By using the relation between the $a_0(980)$-meson wavefunction and its distribution amplitude,

$$\psi_{a_0}(x, \zeta) = \int_{|\boldsymbol{k}_\perp|^2 \leqslant \zeta^2} \frac{{\rm d}^2\boldsymbol{k}_\perp}{16\pi^2}\psi_{a_0}(x, \boldsymbol{k}_\perp). \quad (11)$$

And by combining (4) with (10), one can get the $a_0(980)$-meson leading-twist WF

$$\psi_{a_0}(x, \boldsymbol{k}_\perp) = \frac{m_q^2 A_{a_0}\varphi_{a_0}(x)}{\sqrt{\boldsymbol{k}_\perp^2 + m_q^2}}\exp\left[-\frac{\boldsymbol{k}_\perp^2 + m_q^2}{8\beta_{a_0}^2 x\bar{x}}\right]. \quad (12)$$

We find that the $\sqrt{x\bar{x}}$ in equation (18) has a certain influence on adjusting the LCDA's behavior, so $x\bar{x}$ can be introduced into the longitudinal distribution amplitude, the expression is as follows,

$$\varphi_{a_0}(x) = (x\bar{x})^{\alpha_{a_0}} C_1^{3/2}(2x - 1), \quad (13)$$

where the free parameter α_{a_0} can be obtained by fitting moment $\langle\xi^n_{a_0}\rangle_\zeta$ with the least square method. Furthermore, the $a_0(980)$-meson leading-twist valence-quark distribution function can be obtained by integrating over the squared transverse momentum, i.e. Equation (2), which leads to the following formula

$$q^{a_0}(x, \zeta) = \frac{A_{a_0}^2 m_q^2 (1 - 2x)^2 (x\bar{x})^{2\alpha_{a_0}}}{512\pi^5} \times\left\{{\rm Ei}\left[\sqrt{\frac{m_q^2 + \zeta^2}{4\beta_{a_0}^2 x\bar{x}}}\right] - {\rm Ei}\left[\sqrt{\frac{m_q^2}{4\beta_{a_0}^2 x\bar{x}}}\right]\right\}, \quad (14)$$

with ${\rm Ei}(x) = -\int_{-z}^{\infty}\frac{{\rm e}^{-t}}{t}{\rm d}t$. For further research, the process-independent effective charge is used to redesign the process-dependent-charge alternative and implement evolution to integrate the one-loop Dokshitzer–Gribov–Lipatov–Altarelli–Parisi (DGLAP) equations by describing the evolution of quarks or gluons fragmenting into hadrons and identifying only one hadron at a time. The relevant explanation can be found in [34]. Using this process, one can get the Mellin moments of $a_0(980)$-meson's valence-quark distribution function:

$$\langle x^n q^{a_0}\rangle_\zeta = \int_0^1 x^n q^{a_0}(x, \zeta){\rm d}x. \quad (15)$$

Then, the ratio of Mellin moments is also a point of interest, and its expression is as follows

$$x^n_{a_0}(\zeta, \zeta_k) = \frac{\langle x^n q^{a_0}\rangle_\zeta}{\langle x^n q^{a_0}\rangle_{\zeta_k}}. \quad (16)$$

Another significant physical quantity associated with the $a_0(980)$-meson PDF is its LCDA. The relationship between the $a_0(980)$-meson leading-twist LCDA and the WF is

$$\phi_{a_0}(x, \zeta) = \int_{|\boldsymbol{k}_\perp|^2 \leqslant \zeta^2}\frac{{\rm d}^2\boldsymbol{k}_\perp}{16\pi^3}\psi_{a_0}(x, \boldsymbol{k}_\perp). \quad (17)$$

After integrating over the squared transverse momentum, one can get the LCDA formula

$$\phi_{a_0}(x, \zeta) = \frac{A_{a_0} m_q \beta_{a_0}}{4\sqrt{2}\pi^{3/2}}\sqrt{x\bar{x}}\,\varphi_{a_0}(x) \times\left\{{\rm Erf}\left[\sqrt{\frac{m_q^2 + \zeta^2}{8\beta_{a_0}^2 x\bar{x}}}\right] - {\rm Erf}\left[\sqrt{\frac{m_q^2}{8\beta_{a_0}^2 x\bar{x}}}\right]\right\}, \quad (18)$$

where ${\rm Erf}(x) = 2\int_0^x {\rm e}^{-t^2}{\rm d}x\Big/\sqrt{\pi}$ is the error function. In order to determine the free model parameters A_{a_0}, β_{a_0} and α_{a_0}, we should use the ξ-moments of the $a_0(980)$-meson leading-twist LCDA, which has the following definition

$$\langle\xi^n_{a_0}\rangle_\zeta = \int_0^1 \xi^n \phi_{a_0}(x, \zeta){\rm d}x. \quad (19)$$

On the other hand, the ξ-moments can be calculated by the QCD sum rule approach within background field theory (BFTSR). The two-point correlation function is taken as

$$\Pi^{(n,0)}_{a_0} = {\rm i}\int {\rm d}^4x\, {\rm e}^{{\rm i}q\cdot x}\langle 0|T\{J_n^V(x), J_0^{S,\dagger}(0)\}|0\rangle, \quad (20)$$

with n taking the odd numbers, while the even order will vanish due to the G-parity. The currents are $J_n^V(x) = \bar{q}_1(x)\not{z}({\rm i}z\cdot \overleftrightarrow{D})^n q_2(x)$ and $J_0^S(0) = \bar{q}_1(0)q_2(0)$. The detailed calculation process for the ξ-moments is given in our recent paper [79].

Then, one can adopt the least squares method to fit ξ-moments $\langle\xi^n_{a_0}\rangle_\zeta$ in determining the free model parameters. The purpose of the least squares method is to obtain the optimal value of the fitting parameter θ by minimizing the likelihood function

$$\chi^2(\theta) = \sum_{\rm i=1}^{N}\frac{y_{\rm i} - \mu(x_{\rm i}, \theta)}{\sigma_{\rm i}^2}, \quad (21)$$

where $\mu(x_{\rm i}, \theta)$ is the $a_0(980)$-meson ξ-moments $\langle\xi^n_{a_0}\rangle_\zeta$ of combining equations (18) and (19). The value of $y_{\rm i}$ and its variance $\sigma_{\rm i}$ are defined as the value of ξ-moments calculated by the QCD sum rule. Beyond that, making use of the probability density function $f(y, n_d) = \left(1/\Gamma\left(\frac{n_d}{2}\right)2^{n_d/2}\right)y^{n_d/2-1}e^{-\frac{y}{2}}$ of χ^2, one can get the goodness of fit with the following probability P_{χ^2}

$$P_{\chi^2} = \int_0^1 (f_y;\, n_d)\mathrm{d}y \tag{22}$$

with $P_{\chi^2} \in (0, 1)$. The closer the goodness of fit is to 1, the better the parameters are obtained. Incorporating the effect of scale ζ, according to the renormalization group equations of Gegenbauer moments of the a_0(980)-meson leading-twist LCDA,

$$a_n^{a_0}(\zeta) = a_n^{a_0}(\zeta_0)E_n(\zeta, \zeta_0), \tag{23}$$

where $E_n(\zeta, \zeta_0) = [\alpha_s(\zeta)/\alpha_s(\zeta_0)]^{-(\gamma_n^{(0)}+4)/b}$ and the coefficient $b = (33 - 2n_f)/3$ [46]. n_f is the number of active quark flavors. The ζ_0 and ζ are considered as the initial scale and the running scale. Here we make a notation that the ξ-moments can translate into a a_n-moment directly. The one-loop anomalous dimension is

$$\gamma_n^{(0)} = C_F\left[1 - \frac{2}{(n+1)(n+2)} + 4\sum_{j=2}^{n+1}\frac{1}{j}\right] \tag{24}$$

with $C_F = 4/3$. Then, one can gain the ξ-moments at the arbitrary scales ζ. Then, by fitting moments $\langle\xi_{a_0}^n\rangle_\zeta$ under the different scale ζ with the least square method, LCDA i.e, equation (18) under corresponding scales can be obtained. Finally, according to the wave functions under different scales, we can calculate the a_0(980)-meson valence quark distribution function, Mellin moments $\langle x^n q^{a_0}\rangle_\zeta$ and ratio $x_{a_0}^n(\zeta, \zeta_k)$ with different scales by using equations (2), (15) and (16).

3. Numerical analysis

To do the numerical analysis, the following input parameters are used. The mass of a_0(980)-meson is taken as $m_{a_0} = 0.980 \pm 0.020$ GeV. The current light quark–mass, charm quark mass, the values of the non-perturbative vacuum condensates, the continuum threshold s_0 and the corresponding Borel windows used in ξ-moments BFTSR are consistent with our previous work [79]. Generally, we can treat it as the constituent quark m_q for the a_0(980)-meson with the quark component $q\bar{q}$. In this paper, we take three typical scales, the initial scales $\zeta_0 = 1.0$ GeV, the processes scale $\zeta_2 = 2.0$ GeV and the scale for π-nucleon Drell–Yan experiment [80] or the E615 experiment $\zeta_5 = 5.2$ GeV, which agree with the pion cases [34].

Firstly, based on the sum rule for distribution amplitudes moments $\langle\xi_{a_0}^n\rangle_\zeta$ calculated in our previous work [79], we list the a_0(980)-meson leading-twist LCDA ξ-moments $\langle\xi_{a_0}^n\rangle_\zeta$ with three different scales $\zeta = (1.0, 2.0, 5.2)$GeV in table 1. Here, the accuracy of our calculation is up to the 9th order. It can be seen that the absolute value of ξ-moments decreases as the scale ζ increases. Secondly, the absolute value of ξ-moments decreases as the n increases, which shows that our calculation has good convergence. Then, we adopt the least squares method to fit the ξ-moments $\langle\xi_{a_0}^n\rangle_\zeta$. At the same time, the a_0(980)-meson twist-2 distribution amplitudes with

Table 1. The a_0(980)-meson leading-twist LCDA moments $\langle\xi_{a_0}^n\rangle_\zeta$ at scales $\zeta = (1.0, 2.0, 5.2)$ GeV.

	ζ_0	ζ_2	ζ_5
$\langle\xi_{a_0}^1\rangle_\zeta$	-0.309 ± 0.043	-0.214 ± 0.029	-0.159 ± 0.022
$\langle\xi_{a_0}^3\rangle_\zeta$	-0.184 ± 0.032	-0.093 ± 0.016	-0.049 ± 0.009
$\langle\xi_{a_0}^5\rangle_\zeta$	-0.082 ± 0.027	-0.057 ± 0.017	-0.040 ± 0.011
$\langle\xi_{a_0}^7\rangle_\zeta$	-0.053 ± 0.025	-0.037 ± 0.015	-0.026 ± 0.010
$\langle\xi_{a_0}^9\rangle_\zeta$	-0.043 ± 0.034	-0.014 ± 0.011	0.001 ± 0.005

Table 2. The LCHO model parameters A_{a_0} (in unit: GeV^{-1}), β_{a_0} (in unit: GeV), α_{a_0} and goodness of fit $P_{\chi^2_{\min}}$ changed with the factorization scales $\zeta = (1.0, 2.0, 5.2)$ GeV.

ζ	A_{a_0}	β_{a_0}	α_{a_0}	$P_{\chi^2_{\min}}$
1.0	-203	0.5	-0.55	0.767
2.0	-371	0.5	-0.07	0.865
5.2	-1670	0.5	0.87	0.113

different constituent quarks $m_q = (200, 250, 300, 350)$MeV are shown in figure 1. The result shows that constituent quarks m_q have a certain influence on distribution amplitudes. It is taken to be 250 MeV in the invariant meson mass scheme [81–87] or 330 MeV in the spin-averaged meson mass [89–93]. In this paper, we mainly take $m_q = 250$ MeV. Then, the fitting model parameters with the different scale ζ are given in table 2. Based on the experience of other mesons [69–72, 76, 77, 88, 94, 95], we take the WF model parameter $\beta_{a_0} = 0.5$. Obviously, A_{a_0} gradually decreases with the increment of the scale ζ. However, the goodness of fit $P_{\chi^2_{\min}}$ is not very well when the scale is higher, such as $\zeta = 5.2$ GeV. The reason may lie in the higher-order Gegenbauer moments taking a higher contribution with a larger scale.

With the resultant LCHO model parameters, the curves of a_0(980)-meson leading-twist LCDA with three scales ζ are shown in figure 2. The figure shows that

- The behavior of the three curves tends to be antisymmetric, which will equal zero when the LCDA integrates with respect to x, e.g.

$$\int_0^1 \mathrm{d}x\phi_{a_0}(x, \zeta) = 0. \tag{25}$$

Meanwhile, the three curves go through the zero at the location $x = 0.5$.

- The absolute value of the peaks is decreased with the increase of ζ and the x-location of the peaks tends toward 0.5 with the ζ increase. When the scale tends to infinity i.e. $\zeta \to \infty$, the curve of a_0(980)-meson LCDA will tend to asymptotic form $\phi_{a_0}(x, \infty) = 0$.

Secondly, after taking the LCHO parameters into the a_0(980)-meson valence-quark distribution function, e.g. Equation (14), the predictions of $q^{a_0}(x, \zeta)$ can be obtained.

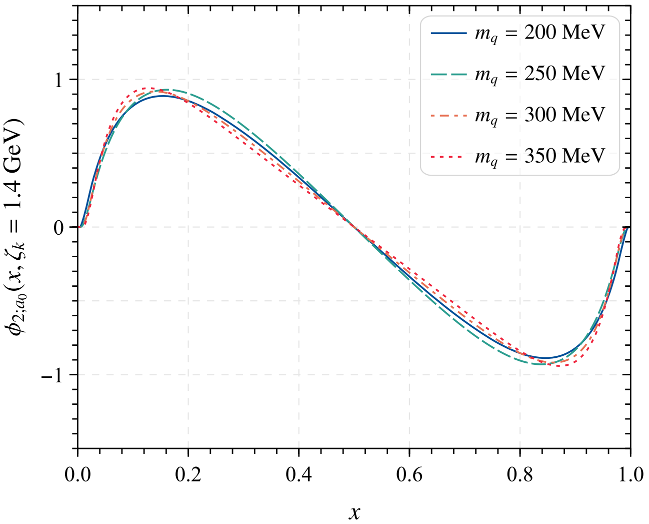

Figure 1. The $a_0(980)$-meson LCDA with different quark masses $m_q = (200, 250, 300, 350)$ MeV.

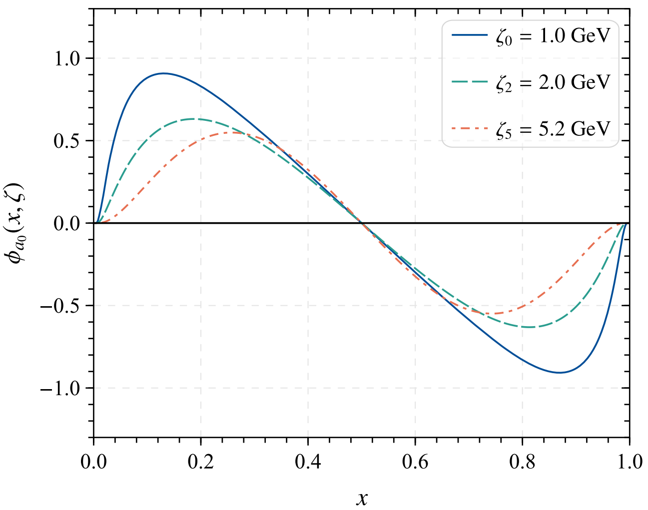

Figure 2. The $a_0(980)$-meson leading-twist LCDA $\phi_{a_0}(x, \zeta)$ changed with three different scales $\zeta = (1.0, 2.0, 5.2)$ GeV.

The curves of $a_0(980)$-meson valence-quark distribution function $q^{a_0}(x, \zeta)$ and $xq^{a_0}(x, \zeta)$ with different scales ζ are shown in figure 3, which shows that the value of peaks decreases with the increase of scale ζ. Since the $a_0(980)$-meson leading-twist LCDA is antisymmetric behavior under the $u \to (1 - u)$ interchange in the $SU_f(3)$ limit, its valence-quark distribution function $xq^{a_0}(x, \zeta)$ tends to zero at $x = 0.5$. Additionally, the valence–quark distribution function tends toward bimodal behavior. In general, the valence-quark distribution functions of pion and kaon tend to a unimodal behavior [34].

Using the meson's valence quark distribution function, we can get the Mellin moments $\langle x^n q^{a_0}\rangle_\zeta$ of the $a_0(980)$-meson valence-quark distribution function, which are presented in table 3. From the table, we can see that the Mellin moments convergence with the order n increased. Meanwhile, the Mellin moments' convergence with the scale ζ increased. This agrees with the Mellin moments of pion's valence-quark distribution function decreasing with the increase of scale. The greater ζ, the smaller the value of the moments in [34]. It proves our prediction of the Mellin moments $\langle x^n q^{a_0}\rangle_\zeta$ is reasonable.

Finally, we also calculate the ratio $x^n_{a_0}(\zeta, \zeta_k)$ of Mellin moments changed with the scale ζ. The predictions of the ratio of Mellin moments with three fixed scales $\zeta_k = (1.0, 2.0, 5.2)$GeV and different orders $n = (1, 2, 3)$ are depicted in figure 4. It is obvious that the $x^n_{a_0}(\zeta, \zeta_k)$ are increased with

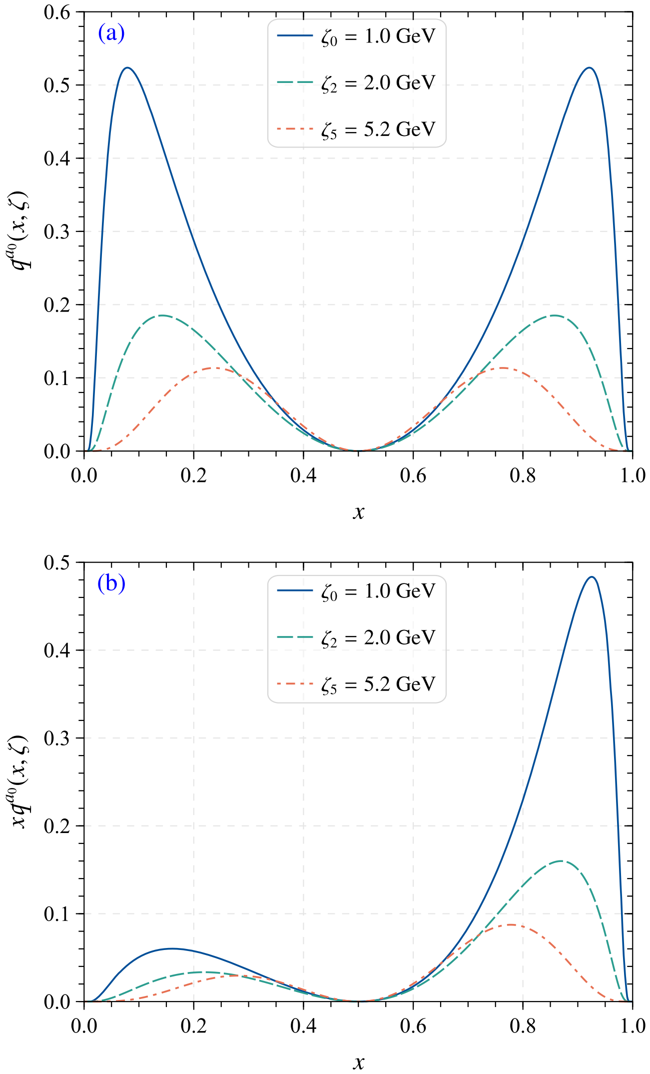

Figure 3. The $a_0(980)$-meson valence quark distribution function $q^{a_0}(x, \zeta)$ and $xq^{a_0}(x, \zeta)$ with different scales.

Table 3. The Mellin moments for $a_0(980)$-meson leading-twist distribution function $\langle x^n q^{a_0}\rangle_\zeta$ with different scales $\zeta = (1.0, 2.0, 5.2)$ GeV.

ζ	$\langle xq^{a_0}\rangle_\zeta$	$\langle x^2q^{a_0}\rangle_\zeta$	$\langle x^3q^{a_0}\rangle_\zeta$
1.0	0.102	0.078	0.065
2.0	0.045	0.032	0.025
5.2	0.027	0.018	0.013

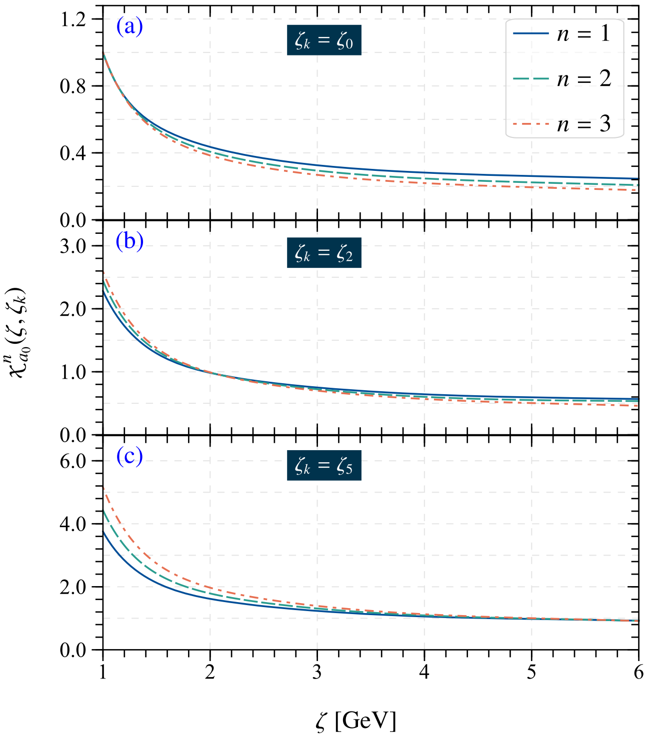

Figure 4. The predicted ratio of Mellin moments of the $a_0(980)$-meson valence-quark distribution function $x^n_{a_0}(\zeta, \zeta_k)$ with three fixed scales $\zeta_k = (1.0, 2.0, 5.2)$ GeV changed with arbitrary scales ζ in the range $\zeta = [1, 6]$ GeV. The n is taken as $n = (1, 2, 3)$ respectively.

index n before the point of ζ_k, and decreased with n after ζ_k. The curves of $x^n_{a_0}(\zeta, \zeta_k)$ are decreasing as the ζ increases. The curves will coincide with each other when the scale ζ and ζ_k tend to infinity.

4. Summary

In this paper, we fit moments $\langle x^n_{a_0}\rangle_\zeta$ with the least squares method to obtain the free model parameters A_{a_0}, β_{a_0} and α_{a_0} at the scales $\zeta = (1.0, 2.0, 5.2)$GeV. Meanwhile, the goodness of fit $P_{\chi^2_{\min}}$ is also given. Then, we present the curves of $a_0(980)$-meson leading-twist LCDA shown in figure 2. After constructing the relationship between $a_0(980)$-meson leading-twist WF and PDFs, the $a_0(980)$-meson valence quark distribution function $q^{a_0}(x, \zeta)$ and $xq^{a_0}(x, \zeta)$ with different scales are shown in figure 3, which tends to bimodal behavior. The LCDA and PDFs tend to zero at the location $x = 0.5$ due to the antisymmetry of the WF. Based on the $a_0(980)$-meson valence quark distribution function, we can get the first three order Mellin moments $\langle xq^{a_0}\rangle_\zeta$ of the $a_0(980)$-meson valence quark DF shown in table 3. Referring to the predicted pion's Mellin moments, our predicted result is quite reasonable. At the same time, we also give the ratio $x^n_{a_0}(\zeta, \zeta_k)$ of Mellin moments with $\zeta = (1.0, 2.0, 5.2)$GeV shown in figure 4. The ratio $x^n_{a_0}(\zeta, \zeta_k)$ shows a downward tendency with the increase of ζ.

Acknowledgments

This work was supported in part by the National Natural Science Foundation of China under Grant No.12265010, No.12265009, the Project of Guizhou Provincial Department of Science and Technology under Grant No.ZK[2021]024, the Project of Guizhou Provincial Department of Education under Grant No.KY[2021]030.

ORCID iDs

Hai-Bing Fu https://orcid.org/0000-0003-2466-6213

References

[1] Collins J C, Soper D E and Sterman G F 1989 Factorization of hard processes in QCD *Adv. Ser. Direct. High Energy Phys.* **5** 1–91
[2] Berger E L and Brodsky S J 1979 Quark structure functions of mesons and the Drell–Yan process *Phys. Rev. Lett.* **42** 940–4
[3] Bjorken J D 1969 Asymptotic sum rules at infinite momentum *Phys. Rev.* **179** 1547–53
[4] Feynman R P 1969 Very high-energy collisions of hadrons *Phys. Rev. Lett.* **23** 1415–7
[5] Bjorken J D and Paschos E A 1969 Inelastic electron proton and gamma proton scattering, and the structure of the nucleon *Phys. Rev.* **185** 1975–82
[6] Gribov V N Space-time description of hadron interactions at high-energies arXiv:hep-ph/0006158
[7] Harland-Lang L A, Martin A D, Motylinski P and Thorne R S 2015 Parton distributions in the LHC era: MMHT 2014 PDFs *Eur. Phys. J.* C **75** 204
[8] Dulat S, Hou T J, Gao J, Guzzi M, Huston J, Nadolsky P, Pumplin J, Schmidt C, Stump D and Yuan C P 2016 New parton distribution functions from a global analysis of quantum chromodynamics *Phys. Rev.* D **93** 033006
[9] Ball R D *et al* (NNPDF) 2017 Parton distributions from high-precision collider data *Eur. Phys. J.* C **77** 663
[10] Alekhin S, Blümlein J, Moch S and Placakyte R 2017 Parton distribution functions, α_s, and heavy-quark masses for LHC run II *Phys. Rev.* D **96** 014011
[11] Ethier J J, Sato N and Melnitchouk W 2017 First simultaneous extraction of spin-dependent parton distributions and fragmentation functions from a global QCD analysis *Phys. Rev. Lett.* **119** 132001
[12] Nam S I 2012 Parton-distribution functions for the pion and kaon in the gauge-invariant nonlocal chiral-quark model *Phys. Rev.* D **86** 074005
[13] Watanabe A, Kao C W and Suzuki K 2016 Meson cloud effects on the pion quark distribution function in the chiral constituent quark model *Phys. Rev.* D **94** 114008
[14] Watanabe A, Sawada T and Kao C W 2018 Kaon quark distribution functions in the chiral constituent quark model *Phys. Rev.* D **97** 074015
[15] Hutauruk P T P, Cloet I C and Thomas A W 2016 Flavor dependence of the pion and kaon form factors and parton distribution functions *Phys. Rev.* C **94** 035201
[16] de Teramond G F *et al* (HLFHS) 2018 Universality of generalized parton distributions in light-front holographic QCD *Phys. Rev. Lett.* **120** 182001
[17] Chang L, Raya K and Wang X 2020 Pion parton distribution function in light-front holographic QCD *Chin. Phys.* C **44** 114105

[18] Watanabe A, Sawada T and Huang M 2020 Extraction of gluon distributions from structure functions at small x in holographic QCD *Phys. Lett.* B **805** 135470
[19] Lan J and Mondal C 2020 Pion-nucleus induced Drell–Yan cross section in models inspired by light-front holography *Phys. Lett.* B **807** 135613
[20] Lan J, Mondal C, Jia S, Zhao X and Vary J P 2019 Parton distribution functions from a light front Hamiltonian and QCD evolution for light mesons *Phys. Rev. Lett.* **122** 172001
[21] Lan J, Mondal C, Jia S, Zhao X and Vary J P 2020 Pion and kaon parton distribution functions from basis light front quantization and QCD evolution *Phys. Rev.* D **101** 034024
[22] Lan J, Mondal C, Jia S, Zhao X, Vary J (BLFQ) *et al* 2020 Light meson parton distribution functions from basis light-front quantization and QCD evolution *Proceedings of the XVIII International Conference Hadron Spectroscopy and Structure* 581–585
[23] Han C, Xing H, Wang X, Fu Q, Wang R and Chen X 2020 Pion valence quark distributions from maximum entropy method *Phys. Lett.* B **800** 135066
[24] Han C, Xie G, Wang R and Chen X 2021 An analysis of parton distribution functions of the pion and the kaon with the maximum entropy input *Eur. Phys. J.* C **81** 302
[25] Chang L, Mezrag C, Moutarde H, Roberts C D, Rodríguez-Quintero J and Tandy P C 2014 Basic features of the pion valence-quark distribution function *Phys. Lett.* B **737** 23–9
[26] Chang L and Thomas A W 2015 Pion valence-quark parton distribution function *Phys. Lett.* B **749** 547–50
[27] Chang L and Roberts C D 2021 Regarding the distribution of glue in the pion *Chin. Phys. Lett.* **38** 081101
[28] Chen C, Chang L, Roberts C D, Wan S and Zong H S 2016 Valence-quark distribution functions in the kaon and pion *Phys. Rev.* D **93** 074021
[29] Shi C, Mezrag C and Zong H S 2018 Pion and kaon valence quark distribution functions from Dyson–Schwinger equations *Phys. Rev.* D **98** 054029
[30] Bednar K D, Cloët I C and Tandy P C 2020 Distinguishing quarks and gluons in pion and kaon parton distribution functions *Phys. Rev. Lett.* **124** 042002
[31] Ding M, Raya K, Binosi D, Chang L, Roberts C D and Schmidt S M 2020 Symmetry, symmetry breaking, and pion parton distributions *Phys. Rev.* D **101** 054014
[32] Freese A, Cloët I C and Tandy P C 2021 Gluon PDF from quark dressing in the nucleon and pion *Phys. Lett.* B **823** 136719
[33] Cui Z F, Ding M, Morgado J M, Raya K, Binosi D, Chang L, Papavassiliou J, Roberts C D, Rodríguez-Quintero J and Schmidt S M 2022 Concerning pion parton distributions *Eur. Phys. J.* A **58** 10
[34] Cui Z F, Ding M, Gao F, Raya K, Binosi D, Chang L, Roberts C D, Rodríguez-Quintero J and Schmidt S M 2020 Kaon and pion parton distributions *Eur. Phys. J.* C **80** 1064
[35] Cui Z F, Ding M, Morgado J M, Raya K, Binosi D, Chang L, De Soto F, Roberts C D, Rodríguez-Quintero J and Schmidt S M 2022 Emergence of pion parton distributions *Phys. Rev.* D **105** L091502
[36] Gao X, Hanlon A D, Karthik N, Mukherjee S, Petreczky P, Scior P, Shi S, Syritsyn S, Zhao Y and Zhou K 2022 Continuum-extrapolated NNLO valence PDF of pion at the physical point *Phys. Rev. D* **106** 114510
[37] Gao X, Jin L, Kallidonis C, Karthik N, Mukherjee S, Petreczky P, Shugert C, Syritsyn S and Zhao Y 2020 Valence parton distribution of the pion from lattice QCD: approaching the continuum limit *Phys. Rev.* D **102** 094513
[38] Gao X, Hanlon A D, Mukherjee S, Petreczky P, Scior P, Syritsyn S and Zhao Y 2022 Lattice QCD determination of the Bjorken-x dependence of parton distribution functions at next-to-next-to-leading order *Phys. Rev. Lett.* **128** 142003
[39] Sufian R S, Egerer C, Karpie J, Edwards R G, Joó B, Ma Y Q, Orginos K, Qiu J W and Richards D G 2020 Pion valence quark distribution from current-current correlation in lattice QCD *Phys. Rev.* D **102** 054508
[40] Lin H W, Chen J W, Fan Z, Zhang J H and Zhang R 2021 Valence-quark distribution of the kaon and pion from lattice QCD *Phys. Rev.* D **103** 014516
[41] Joó B, Karpie J, Orginos K, Radyushkin A V, Richards D G, Sufian R S and Zafeiropoulos S 2019 Pion valence structure from Ioffe-time parton pseudodistribution functions *Phys. Rev.* D **100** 114512
[42] Shugert C, Gao X, Izubichi T, Jin L, Kallidonis C, Karthik N, Mukherjee S, Petreczky P, Syritsyn S and Zhao Y Pion valence quark PDF from lattice QCD arXiv:2001.11650
[43] Izubuchi T, Jin L, Kallidonis C, Karthik N, Mukherjee S, Petreczky P, Shugert C and Syritsyn S 2019 Valence parton distribution function of pion from fine lattice *Phys. Rev.* D **100** 034516
[44] Sufian R S, Karpie J, Egerer C, Orginos K, Qiu J W and Richards D G 2019 Pion valence quark distribution from matrix element calculated in lattice QCD *Phys. Rev.* D **99** 074507
[45] Zhang J H, Chen J W, Jin L, Lin H W, Schäfer A and Zhao Y 2019 First direct lattice-QCD calculation of the x-dependence of the pion parton distribution function *Phys. Rev.* D **100** 034505
[46] Cheng H Y, Chua C K and Yang K C 2006 Charmless hadronic B decays involving scalar mesons: Implications to the nature of light scalar mesons *Phys. Rev.* D **73** 014017
[47] Cheng H Y, Chua C K, Yang K C and Zhang Z Q 2013 Revisiting charmless hadronic B decays to scalar mesons *Phys. Rev.* D **87** 114001
[48] Cheng X D, Li H B, Wei B, Xu Y G and Yang M Z 2017 Study of $\boldsymbol{D} \to a_0(980)e^+\nu_e$ decay in the light-cone sum rules approach *Phys. Rev.* D **96** 033002
[49] Sun Y J, Li Z H and Huang T 2011 $B_{(s)} \to S$ transitions in the light cone sum rules with the chiral current *Phys. Rev.* D **83** 025024
[50] Momeni S and Saghebfar M 2022 Semileptonic D-meson decays to the vector, axial vector and scalar mesons in Hard-Wall AdS/QCD correspondence *Eur. Phys. J.* C **82** 473
[51] Soni N R, Gadaria A N, Patel J J and Pandya J N 2020 Semileptonic decays of charmed mesons to light scalar mesons *Phys. Rev.* D **102** 016013
[52] Jaffe R L 1977 Multi-quark hadrons. 1. The phenomenology of $Q^2\bar{Q}^2$ mesons *Phys. Rev.* D **15** 267
[53] Alford M G and Jaffe R L 2000 Insight into the scalar mesons from a lattice calculation *Nucl. Phys.* B **578** 367–82
[54] Humanic T and (ALICE Collaboration) 2022 Studying the $a_0(980)$ tetraquark candidate using $K_s^0K^{\pm}$ interactions in the LHC ALICE collaboration *Rev. Mex. Fis. Suppl.* **3** 0308039
[55] Brito T V, Navarra F S, Nielsen M and Bracco M E 2005 QCD sum rule approach for the light scalar mesons as four-quark states *Phys. Lett.* B **608** 69–76
[56] Alexandrou C, Berlin J, Dalla Brida M, Finkenrath J, Leontiou T and Wagner M 2018 Lattice QCD investigation of the structure of the $a_0(980)$ meson *Phys. Rev.* D **97** 034506
[57] Klempt E and Zaitsev A 2007 Glueballs, Hybrids, Multiquarks. Experimental facts versus QCD inspired concepts *Phys. Rept.* **454** 1–202
[58] Weinstein J D and Isgur N 1982 Do multi-quark hadrons exist? *Phys. Rev. Lett.* **48** 659
[59] Branz T, Gutsche T and Lyubovitskij V E 2008 $f_0(980)$-meson as a $K\bar{K}$ molecule in a phenomenological Lagrangian approach *Eur. Phys. J.* A **37** 303
[60] Dai L Y, Wang X G and Zheng H Q 2012 Pole analysis of unitarized one loop χPT amplitudes - a triple channel study *Commun. Theor. Phys.* **58** 410–4

[61] Dai L Y and Pennington M R 2014 Two photon couplings of the lightest isoscalars from BELLE data *Phys. Lett.* B **736** 11–5

[62] Sekihara T and Kumano S 2015 Constraint on $K\bar{K}$ compositeness of the $a_0(980)$ and $f_0(980)$ resonances from their mixing intensity *Phys. Rev.* D **92** 034010

[63] Ishida S *et al* 1995 *Proceeding of the 6th International conference on Hadron Spectroscopy (Manchester, UK)*

[64] Ezawa Z F 1974 Wide-angle scattering in softened field theory *Nuovo Cim.* A **23** 271–90

[65] Farrar G R and Jackson D R 1975 Pion and nucleon structure functions near x = 1 *Phys. Rev. Lett.* **35** 1416

[66] Holt R J and Roberts C D 2010 Distribution functions of the nucleon and pion in the valence region *Rev. Mod. Phys.* **82** 2991–3044

[67] Brodsky S J, Huang T and Lepage G P 1983 Particles and fields-2 *Proceedings of the Banff Summer Institute, Ban8; Alberta, 1981* ed A Z Capri and A N Kamal (New York: Plenum) 143

Lepage G P, Brodsky S J, Huang T and Mackenize P B 1983 Particles and fields-2 *Proceedings of the Banff Summer Institute, Ban8; Alberta, 1981* ed A Z Capri and A N Kamal (New York: Plenum) 83

Huang T 1981 *Proceedings of XXth International Conference on High Energy Physics, Madison, Wisconsin, 1980* ed L Durand and L G Pondrom (New York: AIP) 1000 AIP Conf. Proc. No. 69

[68] Zhong T, Wu X G, Wang Z G, Huang T, Fu H B and Han H Y 2014 Revisiting the pion leading-twist distribution amplitude within the QCD background field theory *Phys. Rev.* D **90** 016004

[69] Wu X G, Huang T and Zhong T 2013 Information on the Pion Distribution Amplitude from the Pion-Photon Transition Form Factor with the Belle and BaBar Data *Chin. Phys.* C **37** 063105

[70] Huang T, Wu X G and Zhong T 2013 Finding a way to determine the pion distribution amplitude from the experimental data *Chin. Phys. Lett.* **30** 041201

[71] Huang T, Zhong T and Wu X G 2013 Determination of the pion distribution amplitude *Phys. Rev.* D **88** 034013

[72] Zhong T, Wu X G and Huang T 2016 The longitudinal and transverse distributions of the pion wave function from the present experimental data on the pion–photon transition form factor *Eur. Phys. J.* C **76** 390

[73] Huang T, Wu X G and Wu X H 2004 Pion form-factor in the k_T factorization formalism *Phys. Rev.* D **70** 053007

[74] Wu X G and Huang T 2011 Constraints on the light pseudoscalar meson distribution amplitudes from their meson–photon transition form factors *Phys. Rev.* D **84** 074011

[75] Huang T, Ma B Q and Shen Q X 1994 Analysis of the pion wave function in light cone formalism *Phys. Rev.* D **49** 1490–9

[76] Zhong T, Zhu Z H, Fu H B, Wu X G and Huang T 2021 Improved light-cone harmonic oscillator model for the pionic leading-twist distribution amplitude *Phys. Rev.* D **104** 016021

[77] Hu D D, Fu H B, Zhong T, Wu Z H and Wu X G 2022 $a_1(1260)$-meson longitudinal twist-2 distribution amplitude and the $D \to a_1(1260)\ell^+\nu_\ell$ decay processes *Eur. Phys. J.* C **82** 603

[78] Guo X H and Huang T 1991 Hadronic wave functions in D and B decays *Phys. Rev.* D **43** 2931–8

[79] Wu Z H, Fu H B, Zhong T, Huang D, Hu D D and Wu X G 2023 $a_0(980)$-meson twist-2 distribution amplitude within the QCD sum rules and investigation of $D \to a_0(980)(\to \eta\pi)e^+\nu_e$ *Nucl. Phys. A* **1036** 122671

[80] Conway J S *et al* 1989 Experimental study of muon pairs produced by 252-GeV pions on tungsten *Phys. Rev.* D **39** 92–122

[81] Terentev M V 1976 On the structure of wave functions of mesons as bound states of relativistic quarks *Sov. J. Nucl. Phys.* **24** 106

[82] Jaus W 1990 Semileptonic decays of *B* and *D* mesons in the light front formalism *Phys. Rev.* D **41** 3394

[83] Jaus W 1991 Relativistic constituent quark model of electroweak properties of light mesons *Phys. Rev.* D **44** 2851–9

[84] Chung P L, Coester F and Polyzou W N 1988 Charge form-factors of quark model pions *Phys. Lett.* B **205** 545–8

[85] Choi H M and Ji C R 1997 Relations among the light cone quark models with the invariant meson mass scheme and the model prediction of eta - eta-prime mixing angle *Phys. Rev.* D **56** 6010–3

[86] Schlumpf F 1994 Charge form-factors of pseudoscalar mesons *Phys. Rev.* D **50** 6895–8

[87] Cardarelli F, Grach I L, Narodetsky I M, Salme G and Simula S 1995 Electromagnetic form-factors of the rho meson in a light front constituent quark model *Phys. Lett.* B **349** 393–9

[88] Zhong T, Fu H B and Wu X G 2022 Investigating the ratio of CKM matrix elements $|V_{ub}|/|V_{cb}|$ from semileptonic decay $B_0^s \to K^-\mu^+\nu_\mu$ and kaon twist-2 distribution amplitude *Phys. Rev.* D **105** 116020

[89] Dziembowski Z and Mankiewicz L 1987 Light meson distribution amplitude: a simple relativistic model *Phys. Rev. Lett.* **58** 2175

[90] Dziembowski Z 1988 Relativistic model of nucleon and pion structure: static properties and electromagnetic soft form-factors *Phys. Rev.* D **37** 778

[91] Ji C R and Cotanch S R 1990 Simple relativistic quark model analysis of flavored pseudoscalar mesons *Phys. Rev.* D **41** 2319–22

[92] Ji C R, Chung P L and Cotanch S R 1992 Light cone quark model axial vector meson wave function *Phys. Rev.* D **45** 4214–20

[93] Choi H M and Ji C R 1997 Light cone quark model predictions for radiative meson decays *Nucl. Phys.* A **618** 291–316

[94] Zhong T, Zhang Y, Wu X G, Fu H B and Huang T 2018 The ratio $\mathcal{R}(D)$ and the D-meson distribution amplitude *Eur. Phys. J.* C **78** 937

[95] Zhang Y, Zhong T, Fu H B, Cheng W and Wu X G 2021 D_s-meson leading-twist distribution amplitude within the QCD sum rules and its application to the $B_s \to D_s$ transition form factor *Phys. Rev.* D **103** 114024